Physica Medica 60 (2019) 30–36

Contents lists available at ScienceDirect

Physica Medica

journal homepage: www.elsevier.com/locate/ejmp

Technical note

Dedicated phantom and TLD-100 dosimetry for simultaneous determination of mean glandular dose and beam quality: Proposal for a compact mammography quality control procedure

B. Sánchez-Nieto[a,*], E. López-Pineda[b], C. Ruiz-Trejo[b], I.D. Muñoz[b], P. Caprile[a], G. Chorbadjian[a,c], M.E. Brandan[b]

[a] Instituto de Física, Pontificia Universidad Católica de Chile, Santiago, Chile
[b] Instituto de Física, Universidad Nacional Autónoma de México, 04511 Ciudad de México, Mexico
[c] Subdepartamento de Salud Radiológica, Departamento de Dispositivos Médicos, Instituto de Salud Pública de Chile, Santiago, Chile

1. Introduction

Mammography techniques aimed at the early detection of breast cancer require strict quality control (QC) procedures to assure the generation of images with diagnostic quality [1]. Mammographic images must display high spatial resolution, low noise, high contrast and absence of artifacts. These features must be optimized in relation to the dose imparted to the patient. QC procedures, leading to optimization of image quality with respect to dose [2], include assessment of equipment performance, evaluation of image quality parameters and dosimetry measurements.

The establishment and enforcement of QC regulations is the responsibility of national or local authorities, generally the Ministries of Health. In developing countries, the most severe hardships to a generalized implementation of mammography QC have been limited access to the test equipment and qualified personnel, and incomplete understanding of the benefits that such a program might have in the timely detection of breast cancer. In Latin America, initiatives by organizations such as PAHO and IAEA have promoted the introduction of QC programs via assistance for the acquisition of basic equipment, education and training projects, and publications [3–7].

Authors of this report work at two similarly equipped thermoluminescent (TL) dosimetry laboratories in Chile (CL) and Mexico (MX) universities. The degree of implementation of mammography QC procedures in these countries is different. In Mexico, since 1997 national regulations requiring QC tests have been published, reviewed, and expanded [8–10] and evaluations of clinical image quality and dose have been reported [11,12]. Regulations regarding QC in mammography do not exist in Chile. To our knowledge, only one evaluation of mean glandular dose (MGD) in CL has been published [13].

The MX authors have developed a technique to evaluate MGD and half-value-laver (HVL) using a custom-made phantom (called M3D) [14] that includes calibrated TLD-100 dosimeters. In this way, calibrated ionization chamber (IC) and electrometer, together with high-purity Al foils, are required only for TLD-100 calibration. The original protocol requires deconvolution of the TLD-100 glow curve (GC) into component peaks, which might be a time-consuming complex procedure.

The goals of this study are twofold. Firstly, to optimize the M3D phantom protocol to facilitate the accurate estimation of incident air kerma without scatter (K_i), HVL, and MGD, particularly eliminating the need of the GC deconvolution. Secondly, to define a "compact" mammography QC procedure that includes basic (top-priority) tests and the possible use of the M3D phantom for the dosimetry. The proposed QC procedure, simpler and less labour-intensive than published international comprehensive recommendations [7], has been applied to 5 flat-panel digital systems in each country.

2. Materials and methods

2.1. TL dosimetry laboratories

Participating laboratories were located at Universidad Nacional Autónoma de México, in Mexico City, and Pontificia Universidad Católica de Chile, in Santiago. Equipment at both laboratories consisted of standard annealing ovens, Harshaw-3500 TL readers, and TLD-100(LiF:Ti,Mg) chips ($3.2 \times 3.2 \times 0.89\,mm^3$). The chips were purchased from Thermo Fisher Scientific™ (Waltham, MA, USA) and corresponded to different batches. Previously to this project, both laboratories had implemented weekly tests of their operating conditions performance, thus assuring internal reproducibility of measurements.

2.2. Reference dosimetry systems

Reference dosimetry systems were based on ICs: A Radcal 20X6-6M (cross-calibrated to an Exradin A2 calibrated at the National Institute of

* Corresponding author.
E-mail address: bsanchezn@fis.puc.cl (B. Sánchez-Nieto).

https://doi.org/10.1016/j.ejmp.2019.03.018
Received 11 September 2018; Received in revised form 24 January 2019; Accepted 19 March 2019
Available online 23 March 2019

Standards and Technology, NIST) connected to a Radcal 2026C electrometer in MX; and a PTW TN23344 connected to an IBA DOSE 1 Electrometer, both calibrated by the University of Wisconsin-Radiation Calibration Laboratory, in CL.

2.3. Standardized procedure for TLD-100 use

To achieve the goals of this study, both laboratories had to standardize (i.e., to make mutually consistent) their TLD-100 dosimeter protocols. During this process, the GC deconvolution, originally required to identify contributions from individual peaks and to eliminate unwanted signals from the TL integral [14], was eliminated. Since only the integral of the TL signal was required for the M3D phantom, annealing and reading protocols were adjusted to offer results equivalent to the GC deconvolution. Addition of a pre-reading annealing reduced the contribution from low-temperature peaks and lowering the maximum temperature in the reading stage minimized the GC planchet signal.

The joint protocol for TLD-100 preparation was as follows. One-hour pre-irradiation annealing at 400 °C was followed by rapid cooling at room temperature for 15 min; then, 2 h at 100 °C followed by the same cooling procedure. Irradiation took place at least 24 h after completing the annealing. Readout, performed at least 24 h after exposure, started with a pre-reading annealing at 100 °C for 10 min followed by rapid cooling. The TL signal was acquired at 8 °C s^{-1} from zero to 320 °C under controlled high-purity nitrogen flow. The GC was integrated and the background signal from non-irradiated dosimeters was subtracted, yielding the net TL signal.

In order to quantify possible systematic differences due to operational conditions of both TL readers (mainly, applied voltages and light reflection from the planchet), ten dosimeters from a reference batch were exposed together to mammography X-rays, then divided into two groups and finally read simultaneously by each laboratory (control TLDs were used to account for any extra dose – e.g., from cosmic radiation- while in transit). Net TL signals were compared to obtain a cross-factor. Additionally, possible inter-batch differences were evaluated by exposing at both sites dosimeters from the local and reference batches and comparing their signals.

Finally, consistency between measurements performed at both facilities was evaluated measuring a “basic physics” process: the TLD-100 sensitivity to air-kerma (F_K, TL signal divided by K_i) as a function of beam quality. This was studied at each laboratory independently by exposing chips from both laboratories to different mammography beams and using the joint protocol. Air-kerma at the point of exposure and HVL (from 0.37 to 0.56 mm Al) were determined [7] by the reference dosimetry equipment available locally. The F_K values determined at both sites were compared to a monoenergetic analytical calculation of X-ray energy deposition in 0.89 mm of LiF.

2.4. The M3D phantom

The 4.5 cm thick PMMA M3D phantom developed in MX [14] (equivalent to a 53 mm thick breast, 29% glandularity [7]) was reproduced in CL (Fig. 1) and used to assess K_i, HVL and MGD. The M3D carries 15 TLD-100 chips under a 5 mm thick PMMA top plate. The response of 3 of the chips (“kerma TLDs”) was used to determine K_i; the other 12 chips (“HVL TLDs”), located under four Al foil thicknesses, were used to determine HVL. Before use, M3D required calibration under various known beam qualities, as described in [14]. Expressions to calculate the three magnitudes are briefly described.

The energy-dependent calibration coefficient, L_Q, relates K_i (determined by an IC) to the kerma TLDs signal, M_k, by

$$K_i = L_Q M_k \quad (1)$$

Correction factors, L_C, are applied to the HVL TLDs signal, M_{HVL}, to account for differences in scattering between in-phantom and in-air measurement conditions, as

$$M'_{HVL} = L_C M_{HVL} \quad (2)$$

HVL is then obtained from the M'_{HVL} values determining the Al thickness that reduces M'_{HVL} to one-half, as it is done with IC measurements. Finally, MGD is calculated following [15], as

$$MGD = g_t c_t s K_i \quad (3)$$

where g_t converts K_i to MGD for a breast t mm thick and 50% glandular, and c_t corrects for glandularity different from 50%. Both parameters depend on HVL and breast thickness. The s factor corrects for anode/filter combinations different from Mo/Mo. Values for these parameters are tabulated in [15,16].

In this work, the M3D was calibrated (i.e., L_Q and L_c were determined) by each laboratory for a range of clinically relevant beam qualities, including target/filter combinations Mo/Mo, Mo/Rh, Rh/Rh, W/Rh, W/Al and W/Ag, and 24–31 kV operating voltage values.

For the application of M3D to dosimetry QC procedures, a twin phantom (same material and geometry but without TLDs holders nor Al filters) was built and used to determine the clinical irradiation conditions (AEC technique) for the phantom. In order to test the M3D ability to determine K_i, HVL and MGD, measurements of these magnitudes were compared to IC measurements performed under the same irradiation conditions.

2.5. Quality control tests

National regulations to evaluate the technical performance of mammography systems are generally based on international recommendations. In Latin America, recommendations by the IAEA [7], the Spanish Medical Physics Society [17,18] and the American College of Radiology [19] are probably the most frequently followed. A set of basic tests (and their compliance requirements) were selected from these recommendations [7,17–19]. The goal was to limit the choice to tests considered essential, considering the limited availability of local resources (equipment, personnel and clinical X-ray beam time). This QC proposal is composed by 12 tests that addressed four categories: general equipment performance, image quality, digital detector and dosimetry performance. Table 1 lists the tests.

General equipment performance (T1-T3) included visual and mechanical evaluation of the unit (mechanical stability, angulation and light indicators and fluidity in the movements [7,19]) and mechanical and manual measurement of the compression force [18,19]. Automatic Exposure Control (AEC), repeatability of the signal-to-noise ratio (SNR) and the mAs were verified using a 4.5 cm thick “standard” PMMA homogeneous phantom [18]. AEC compensation for four PMMA thicknesses (T4) was verified measuring contrast-to-noise ratio (CNR) of a 0.2 mm thick, 1 cm × 1 cm, 99%-purity Al foil piece [18]. The AEC-chosen technique for the 4.5 cm thick standard PMMA phantom is referred to as the “clinical conditions”.

Image quality aspects (T5-T7) included response inhomogeneities of the image receptor caused by deficiencies or inadequate corrections during the flattening process. Raw images of the PMMA phantom were used and mean-pixel-values (MPV) and their standard deviation were measured in 5 regions-of-interest (ROI); the presence of artifacts was evaluated visually on standard phantom images acquired under clinical conditions [18]. Limiting spatial resolution was evaluated using a bar resolution pattern on the standard phantom, under clinical conditions [7,19]. Image quality was evaluated using two phantoms: the ACR Mammography Accreditation Phantom [19] developed for conventional mammography and widely used in Latin America, and the digital contrast-detail CDMAM 3.4 phantom [20], used mostly in Europe. Image phantom tests were performed following the published instructions [19,18]. CDMAM tests were analysed with the Artinis Analyser V1.2.1 (CL) and CDMAM Analysis V1.5.5 (MX) tools.

Performance of the digital detector (T8-T9) was assessed measuring

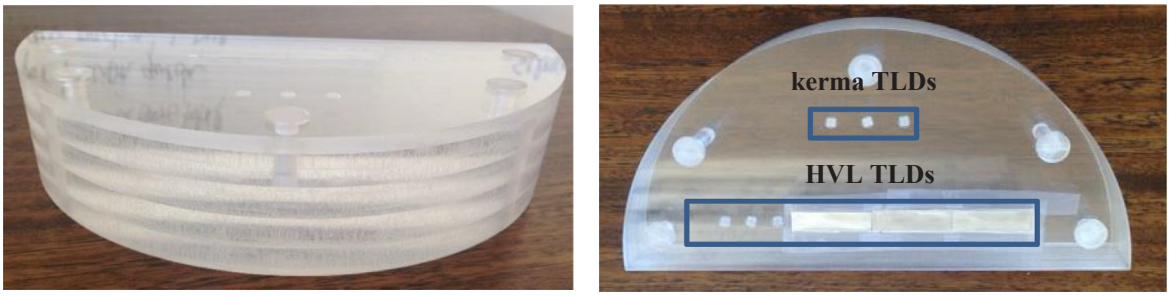

Fig. 1. M3D mammographic phantom manufactured in CL, a duplicate of the original phantom presented in [16]. Lateral (left) and upper (right) views. On the right view, labels show the "kerma TLDs" and "HVL TLDs". Only 3 out of the 12 HVL TLDs can be identified, since the rest is located under the Al foils.

the response function to incident air-kerma in images of the standard phantom for different mAs [18]. These images were also used to determine the source of noise fitting the typical pixel deviation (TPD) (noise) as a power function of incident kerma [17].

Evaluation of the dosimetry performance (T10-T12), required measurement of the tube output (mGy/mAs) under clinical conditions, HVL and MGD [7,18]. HVL and MGD were determined using an IC [7,18,19]. MGD was calculated from air kerma [18] following the formalism in [15,16].

HVL and MGD tests traditionally require the use of an IC, as indicated above. As part of this work (and based on results from [14]), we are proposing an alternative procedure using the M3D phantom (Section 2.4). The justification is reducing time and complexity when performing these tests. In this work, we compared measurements of HVL, K_i and MGD using both methods for the imaging parameters corresponding to the AEC technique for the M3D phantom.

2.6. Application of the proposed QC protocol

Five clinical mammography units were evaluated (tests in Table 1) in each country and Table 2 lists their main characteristics.

For HVL (T11) and MGD (T12), due to the limited beam time assigned for the evaluation by the clinical services in CL, it was only possible to measure for the 4.5 cm PMMA thickness. In MX, the complete proposed protocol in Table 1 was applied.

3. Results and discussion

3.1. TLD-100 standardized procedure

As expected after application of a common dosimeter annealing and reading protocol, TLD-100 GC from both laboratories exhibited similar shape. Fig. 2 shows typical GC obtained for chips from the same batch exposed together and read simultaneously at each laboratory. The average relative TL intensity of readings performed at MX with respect to CL ("cross-factor") was 0.97 ± 0.03. The difference could be mainly due to differences in the photomultipliers' gain. Remaining minor GC shape discrepancies might be attributed to the planchet conditions. Additionally, no statistically significant inter-batch differences were found.

Fig. 3 displays the TLD-100 sensitivities to air-kerma for spectra characterized by their effective energy. Results obtained at the two laboratories agree, within uncertainties, and the energy dependence displayed by measurements is well described by the calculation. These data represent the TLD-100 energy-dependent response.

3.2. M3D phantom calibration and application

Fig. 4 shows calibration factors L_Q calculated by each laboratory for beams characterized by HVL. As observed, the values and energy-dependence are similar. Smaller uncertainties in Fig. 4a) with respect to Fig. 4b) are due to the larger number of chips used at the MX

Table 1
Compact QC protocol.

Category	Test	Requirement
General equipment performance	T1. Mechanical and visual evaluation	Checked elements must be in good shape and/or perform appropriately.
	T2. Compression force	Motorized compression must be 111 − 200 N; manual compression must be less than 300 N. Nominal and measured compression must agree within 20 N.
	T3. AEC repeatability	SNR maximum deviation from mean = 5%; mAs maximum deviation from mean = 5%.
	T4. AEC compensation for breast thickness and glandularity	For each phantom thickness (3.0, 4.5, 5.0 and 6.0 cm), the percentage relative CNR (relative to the threshold thickness of the 0.1 mm disk –see T7) must be equal to or larger than the limit values.
Image quality	T5. Image uniformity and artifacts	MPV maximum deviation in individual (5) ROIs < ± 15%. SNR maximum deviation of individual (5) ROIs < ± 20%. No artifacts in the image.
	T6. Spatial resolution	Spatial resolution as close as possible, and always larger than 80% of the Nyquist frequency associated to the detector pixel size.
	T7. Image quality using a phantom	Visualization of objects or contrast thresholds, according to the available accredited phantom. For ACR, the minimum number of fibres, masses and calcifications are 4, 3 and 4, respectively. For CDMAM, the threshold thickness of the 0.1, 0.25, 0.5, 1, and 2 mm gold disks are 1.68, 0.352, 0.150, 0.091 and 0.069 μm, respectively.
Digital detector performance	T8. Response function	Linear MPV as a function of entrance surface kerma, $R^2 > 0.99$.
	T9. Noise exponent	When fitting TPD = a $(Ki)^b$, exponent b = 0.50, tolerance ± 0.05.
Dosimetric performance	*T10. Output under clinical conditions	No limit value, measurements taken as reference.
	*T11. Half-value-layer (HVL)	kV/100 + 0.03 < HVL(mmAl) < kV/100 + C.
	*T12. Mean glandular dose (MGD)	MGD ≤ 1.5 mGy, 2.5 mGy, 3 mGy and 4.5 mGy for the 3.0, 4.5, 5.0 ad 6.0 cm phantom thicknesses, respectively.

* These tests were applied using the conventional procedure based on the ionization chamber as well as using the M3D phantom (procedure in Section 2.4 and [14]).

Table 2
Evaluated mammography units. Identification code ID indicates the unit location, MX and CL.

ID	Manufacturer and model	Anode;filters	Image receptor	Pixel size (μm)
MX_1	Hologic Selenia Dimensions	W;Rh, Ag, Al	DirectRay FFDM-SD	70
MX_2	Hologic Lorad Selenia	Mo;Mo, Rh	DirectRay FFDM-L	70
MX_3	FUJIFILM Amulet Innovality	W;Rh, Al	FUJIFILM	50
MX_4	FUJIFILM Amulet Innovality	W;Rh, Al	FUJIFILM	50
MX_5	Giotto Image 3DL	W;Ag	IMS	85
CL_1	Siemens Mammomat Inspiration	W, Mo;Mo, Rh	Eleman 2	85
CL_2	GE Senographe Essential	Mo, Rh;Mo,Rh	GE	100
CL_3	GE Senographe Essential	Mo, Rh;Mo,Rh	GE	100
CL_4	GE Senographe Essential	Mo, Rh;Mo,Rh	GE	100
CL_5	Hologic Selenia Dimensions	W;Rh, Ag, Al	DirectRay FFDM	70

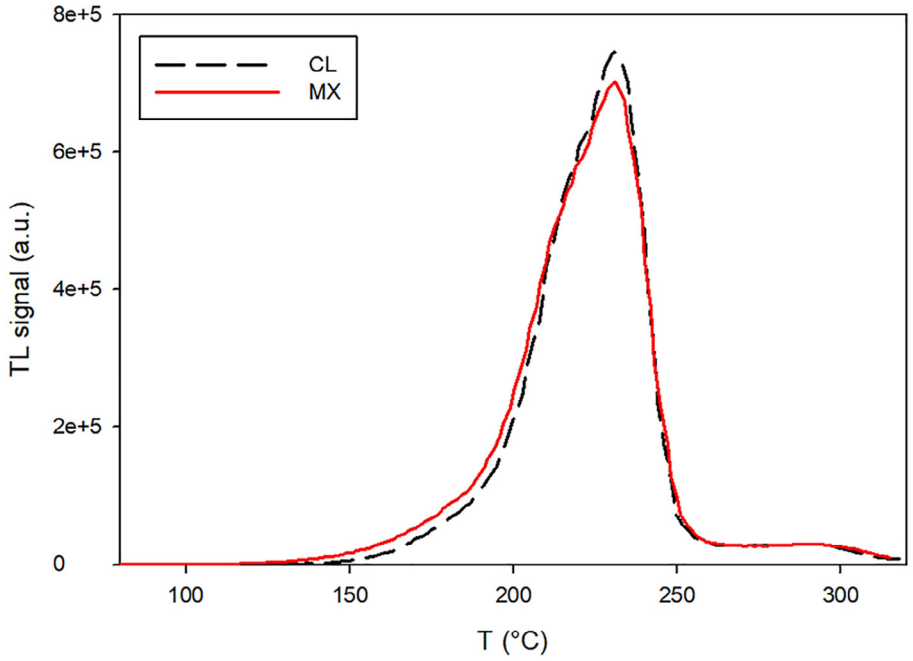

Fig. 2. TLD-100 glow curves for chips from the same batch, irradiated together, and simultaneously read at each laboratory.

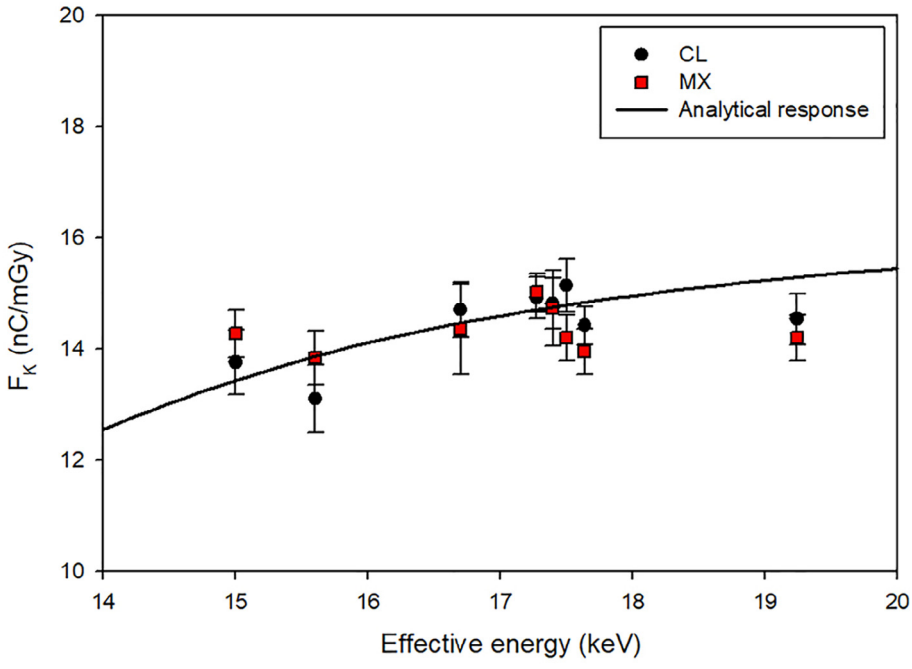

Fig. 3. Air kerma sensitivity as function of effective energy. Effective energies were calculated from the measured HVL. TLDs were irradiated and read by each laboratory. Squares and circles correspond to data from MX and CL, respectively. The latter were multiplied by the cross factor 0.97 to match reader response. Each data point is the average of 4 dosimeters and the error bars correspond to one standard deviation. The solid line shows an analytical prediction of the response of LiF as a function of energy (normalized to point value from MX at 15.6 keV).

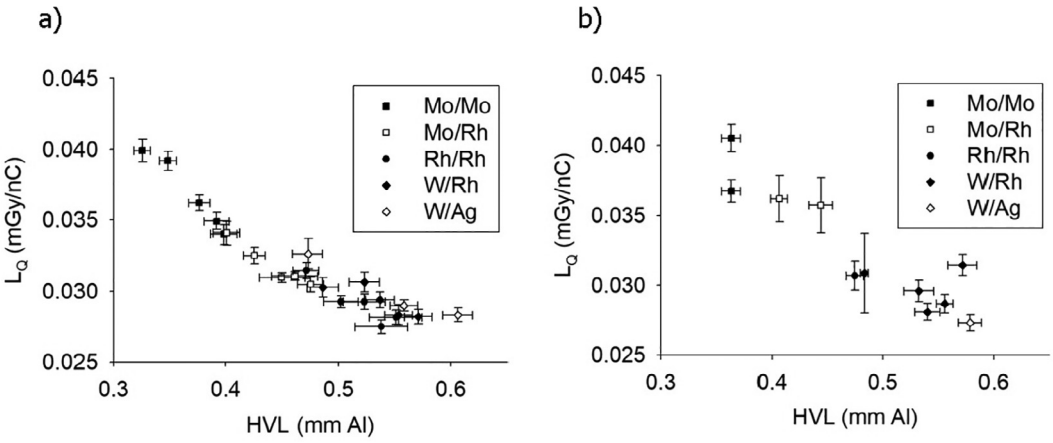

Fig. 4. Calibration coefficients, L_Q, as a function of HVL, evaluated in MX (a) and CL (b).

laboratory. Since the relative TL response per unit kerma has been verified previously (Fig. 3), one can argue that the small differences observed between L_Q values in Fig. 4 for the two laboratories could arise from the use of different M3D phantoms (materials acquisition and machining were done locally). Measurements were performed to test this hypothesis[1]. However, differences found between materials did not explain the discrepancies. Moreover, as long as each laboratory makes use of their own calibration curve together with the phantom, these differences should not affect the MGD determination.

Table 3 displays results for K_i, HVL, and MGD determined by the IC and the M3D phantom. As expected, uncertainties after the use of TL dosimetry were larger than for ICs. The mean relative values of phantom to IC measurements were 0.99 ± 0.06 (k = 1 for the combined standard uncertainty), 1.01 ± 0.07 (k = 1), and 0.99 ± 0.09 (k = 1) for K_i, HVL, and MGD, respectively. Thus, no systematic difference was observed between measurements of these quantities performed by the two methods in both laboratories (consistent with previous results using GC deconvolution [21]). We consider that this result validates the possible use of the M3D phantom in routine mammography QC.

3.3. QC tests and application

Tables 4a–c show the results of the tests. Only results for 4.5 cm PMMA are reported in T4, T10, T11, and T12. Check marks (pass) or crosses (fail) have been added to indicate compliance (or lack of) with requirements (Table 1). Nine out of 12 tests were passed by all the units. Three out of 10 units (all in CL) passed all the tests.

Table 4a shows results for the T1-T4 tests. T1, T3, and T4 were passed by all the units. Moreover, T4 was passed for the 4 tested PMMA thicknesses. All the units in MX failed compression force (T2) tests due to a systematic disagreement larger than 20 N between measured and nominal applied force under manual and motorized operation. One of these units also failed to show the expected stability in the compression. Stability could not be measured in CL units due to features of the available scale.

Table 4b displays results for the image quality tests. T6 and T7 were passed by all the units. Regarding the last one, only thresholds for the thinnest gold disks of 0.1 mm are reported but 0.25, 0.5, 1 and 2 mm thickness were also satisfactorily tested in all units. T5 was unsatisfactory in 3 of the MX units, where the SNR showed deviations from the mean larger than the 20% tolerance.

With relation to image quality measured with the CDMAM, the protocol originally considered use of two different software packages for the automatic evaluation of contrast thresholds. However, these are not equivalent since Artinis Analyser V1.2.1 determines the thresholds based on the automatic image readout, while CDMAM Analysis V1.5.5 includes a transformation from automatic values into what would be determined by human observers. For internal consistency, we analyzed the phantom images with both codes, and report only results obtained with CDMAM Analysis V1.5.5. The ratio of the predicted human to automatic threshold gold thickness, for the 0.1 mm disk in CDMAM, was 1.46 ± 0.12 (k = 1), consistent with Ref. [22].

Table 4c shows results for digital detector and dosimetry performance evaluated with an IC. T9 was acceptable in 8 out of 10 units, indicating dominance of Poisson noise. The exponent measured in the non-compliant units indicated excessive contribution from structured noise. All units showed the expected linear detector response as function of entrance kerma, as well as acceptable values for HVL and MGD for 4.5 cm PMMA under clinical conditions.

For a given set of imaging parameters, using the M3D phantom instead of the IC to measure HVL and K_i (the two measurements needed to evaluate MGD) resulted in significant time savings, from about 45 min (typically, 15 irradiations when using the IC) down to 5 min (3 irradiations, when using the phantom). This large time-reduction, together with the excellent agreement between the results with the two methods, should be considered as a remarkable advantage of the M3D phantom over the traditional IC. In developing countries, medical physicists encounter limited beam time assigned by the hospital to perform the QC tests, and savings of this magnitude could represent the difference between performing –or not– the required dosimetry.

The European Federation of Organisations for Medical Physics (EFOMP) recently defined a QC protocol in digital mammography containing the minimum set of high-priority tests (12) to assure the performance of a system [2]. Most of our selected tests (except T1, T2, and T6) are those suggested by EFOMP. This agreement can be interpreted as a strength of our proposal.

4. Conclusions

The joint TL dosimetry protocol enabled to measure similar TL responses for a broad range of mammography beam qualities in both laboratories. The simplified TL protocol made dosimetry evaluations more robust, simpler, and less user-dependent and yielded results for K_i, HVL, and MGD in good agreement with IC determinations.

[1] To identify possible differences in their composition, samples of PMMA used in the two phantoms were subjected to Raman spectroscopy and density measurements. Raman spectroscopy revealed differences in the polymer tacticity. The sample from CL showed Raman bands (2636 cm^{-1} and 3454 cm^{-1}) compatible with a syndiotactic form (of crystalline nature) whereas the sample from MX seemed to be more amorphous. These results are consistent with the larger mass density measured in the PMMA from CL (1.186 ± 0.002 g/cm^3) than the PMMA from MX (1.166 ± 0.007 g/cm^3).

Table 3
Dosimetry results (K_i, HVL, and MGD) obtained with IC and the M3D phantom for the clinical irradiation conditions for the M3D phantom.

	K_i (IC) [mGy]	K_i (phantom) [mGy]	HVL (IC) [mm Al]	HVL (phantom) [mm Al]	MGD (IC) [mGy]	MGD (phantom) [mGy]
MX_1	4.36 ± 0.05	4.1 ± 0.2	0.50 ± 0.03	0.48 ± 0.03	1.22 ± 0.07	1.11 ± 0.08
MX_2	10.55 ± 0.12	9.1 ± 0.4	0.37 ± 0.02	0.39 ± 0.03	2.18 ± 0.13	1.94 ± 0.15
MX_3	4.84 ± 0.05	5.0 ± 0.2	0.56 ± 0.02	0.59 ± 0.02	1.51 ± 0.08	1.66 ± 0.09
MX_4	4.84 ± 0.05	4.4 ± 0.2	0.53 ± 0.03	0.50 ± 0.03	1.43 ± 0.08	1.24 ± 0.09
MX_5	5.02 ± 0.06	5.3 ± 0.3	0.59 ± 0.03	0.54 ± 0.07	1.66 ± 0.12	1.60 ± 0.21
CL_1	10.4 ± 0.2	10.6 ± 1.4	0.43 ± 0.01	0.41 ± 0.02	2.48 ± 0.05	2.43 ± 0.33
CL_2	5.6 ± 0.1	5.7 ± 0.8	0.44 ± 0.01	0.49 ± 0.05	1.40 ± 0.03	1.45 ± 0.23
CL_3	4.1 ± 0.1	4.0 ± 0.5	0.44 ± 0.01	0.46 ± 0.04	1.03 ± 0.02	1.05 ± 0.14
CL_4	5.3 ± 0.1	5.1 ± 0.7	0.44 ± 0.01	0.49 ± 0.05	1.35 ± 0.03	1.16 ± 0.20
CL_5	3.8 ± 0.1	4.0 ± 0.6	0.52 ± 0.01	0.50 ± 0.05	1.11 ± 0.02	1.05 ± 0.14

Table 4a
Results for general equipment performance tests. For T4, only results for 4.5 cm thick PMMA are reported.

Unit ID	T1. Mechanical and visual evaluation	T2. Compression force						T3. AEC repeatability		T4. AEC compensation
		Manual [N]			Motorized [N]					
		Nominal	Measured	Stability	Nominal	Measured	Stability	mAs variability (%)	SNR variability (%)	Measured (Limit) CNR
MX_1	✓	250	226 ×	0✓	190	167×	0✓	2.8✓	1.3✓	6.8 (4.7)✓
MX_2	✓	320	285 ×	0✓	180	137×	0✓	0.6✓	1.8✓	6.4 (3.6)✓
MX_3	✓	210	177×	0✓	200	157×	0✓	0✓	0.7✓	4.9 (2.2)✓
MX_4	✓	240	206×	0✓	200	157×	0✓	0.5✓	2.5✓	6.5 (3.7)✓
MX_5	✓	170	137×	1 ×	180	137×	1 ×	0.6✓	1.7✓	8.4 (6.1)✓
CL_1	✓	200	201✓	NA	200	199✓	NA	1✓	0.5✓	10.6 (5.5)✓
CL_2	✓	200	201✓	NA	170	168✓	NA	0.7✓	1.6✓	12.1 (10.6)✓
CL_3	✓	170	169✓	NA	180	169✓	NA	0✓	0.5✓	9.2 (8.1)✓
CL_4	✓	220	209✓	NA	180	171✓	NA	0.9✓	2.4✓	0.3 (0.2)✓
CL_5	✓	170	154✓	NA	160	147✓	NA	4.9✓	1.3✓	6.8 (3.8)✓

Table 4b
Results for image quality tests.

Unit ID	T5. Image uniformity and artifacts			T6. Spatial resolution	T7. Image quality with phantom	
	MPV max deviation	SNR max deviation	Artifacts	Line pairs (Limit value)	CDMAM threshold for 0.1 mm [μm]	ACR score
MX_1	0.3✓	17.2✓	No✓	10 (5.7)✓	1.12 ± 0.12✓	14✓
MX_2	0.8✓	16.0✓	No✓	10 (5.7)✓	1.20 ± 0.14✓	14✓
MX_3	1.5✓	21.7 ×	No✓	10 (8.0)✓	1.01 ± 0.13✓	15✓
MX_4	9.9✓	25.4 ×	No✓	9 (8.0)✓	1.01 ± 0.13✓	14✓
MX_5	9.9✓	25.4 ×	No✓	8 (4.7)✓	1.25 ± 0.15✓	14✓
CL_1	4.5✓	3.3✓	No✓	6 (4.7) ✓	0.90 ± 0.10✓	13✓
CL_2	5.3✓	16.3✓	No✓	7 (4.0) ✓	1.24 ± 0.15✓	15✓
CL_3	3.0✓	2.5✓	No✓	7 (4.0) ✓	1.54 ± 0.18✓	12✓
CL_4	6.0✓	3.0✓	No✓	7 (4.0) ✓	1.26 ± 0.15✓	13✓
CL_5	2.8✓	3.5✓	No✓	NA (5.7)	0.80 ± 0.09✓	14✓

This study proposed a compact QC protocol for mammography, which evaluates the basic performance of the equipment, including dose and image quality. The application of the protocol to 10 digital mammography units showed that they were generally performing according to the requirements of the proposed compact set of tests.

Considering that the evaluated units in CL were not subjected to regular QC (additional to technical maintenance), their relatively good performance were unexpected results. A previous independent evaluation of MGD in clinical mammographic units in CL [13] had found values outside compliance levels for the 4.5 cm PMMA reference phantom. In this evaluation, all the units complied with limit values, possibly due to the relatively new (manufactured after 2014) equipment pool included in this study. This interpretation is consistent with recent results [23] in Mexican flat-panel units tested at commissioning.

As expected, the replacement of IC-based tests by a TLD-based phantom reduced time and human and equipment resources needed for determination of dosimetry performance parameters (at the cost of

Table 4c
Results for digital detector and dosimetry performance. For T10-T12, only results for 4.5 cm PMMA are reported.

Unit ID	T8. Response function linearity (r^2)	T9. Noise exponent	T10. Output at clinical conditions		T11. Half-value layer [mm Al]	T12. Mean glandular dose [mGy]
			AEC clinical conditions (anode/filter/kV)	Output [mGy/mAs]		
MX_1	0.9999✓	0.49✓	W/Rh/29	0.0362 ± 0.0003	0.50 ± 0.03✓	1.22 ± 0.07✓
MX_2	0.9999✓	0.55✓	Mo/Mo/29	0.1380 ± 0.0012	0.37 ± 0.02✓	2.18 ± 0.13✓
MX_3	0.9999✓	0.47✓	W/Rh/29	0.0485 ± 0.0004	0.56 ± 0.02✓	1.51 ± 0.08✓
MX_4	0.9999✓	0.50✓	W/Rh/29	0.0542 ± 0.0005	0.53 ± 0.03✓	1.43 ± 0.08✓
MX_5	0.9999✓	0.55✓	W/Ag/29	0.0708 ± 0.0006	0.59 ± 0.03✓	1.66 ± 0.12✓
CL_1	0.9958✓	0.47✓	Mo/Rh/29	0.092 ± 0.002	0.44 ± 0.01✓	2.42 ± 0.05✓
CL_2	0.9946✓	0.69×	Rh/Rh/29	0.090 ± 0.002	0.47 ± 0.01✓	1.53 ± 0.03✓
CL_3	1.0000✓	0.58×	Mo/Rh/27	0.076 ± 0.002	0.41 ± 0.01✓	1.18 ± 0.02✓
CL_4	0.9962✓	0.55✓	Rh/Rh/29	0.092 ± 0.002	0.44 ± 0.01✓	1.38 ± 0.03✓
CL_5	0.9972✓	0.48✓	W/Rh/28	0.036 ± 0.001	0.53 ± 0.01✓	1.16 ± 0.02✓

higher uncertainties). Specifically, X-ray output of tube, HVL and MGD could be determined with few exposures of the M3D phantom. The inclusion of thicknesses other than 4.5 cm would require additional plates into M3D, different sets of TLDs previously loaded, and an extension of the calibration.

This study constitutes a first complete evaluation of operating conditions of mammography equipment in CL and should help actions leading to national regulations for image quality and dose. We believe that centres without access to an IC and its electrometer, experienced personnel needed to handle them onsite, or sufficient time for QC tests, would benefit from the use of the M3D phantom as an alternative to the dosimetry tests. Nonetheless, this QC strategy requires of well-equipped national metrology laboratories with well-trained personnel. This could ease the adoption, in some facilities, of a QC culture in mammography.

Acknowledgements

Contribution to data acquisition by G. Zelada, V. Aguirre, M.P. Durán, P. Espinoza, P. Sandrock, C. Muñoz, J. Espino, M.A. Nava, and H. Galván is appreciated. We thank I. Gamboa-deBuen for advice and calculations, and A. Cabrera for measurements and discussions on PMMA properties. Project partially funded by a CONICYT, Chile–CONACYT (Mexico) binational grant (PCCI130006 in Chile and C0005-2013-01 205371 in Mexico). The Mexican team acknowledges partial funding from DGAPA-UNAM Grant IN107916. BS acknowledges Fondecyt Regular N1181133 and Puente P1702/2017.

References

[1] World Health Organization. WHO position paper on mammography screening. Switzerland: WHO Press; 2014.
[2] Gennaro G, Avramova-Cholakova S, Azzalini A, Chapel ML, Chevalier M, Ciraj O, et al. Quality controls in digital mammography protocol of the EFOMP mammo working group. Phys Med 2018;48:55–64.
[3] OPS. Mammography Services Quality Assurance: Baseline Standards for Latin America and the Caribbean. PAHO 2016.
[4] Jiménez P, Borrás C, Fleitas I. Accreditation of diagnostic imaging services in developing countries. Pan Am J Public Heal 2006;20:104–12.
[5] Mora P, Khoury H, Bitelli R, Quintero AR, Garay F, Aguilar JG, et al. Latin American image quality survey in digital mammography studies. Radiat Prot Dosimetry 2017;174:94–101.
[6] Mora P, Faulkner K, Mahmoud AM, Gershan V, Kausik A, Zdesar U, et al. Improvement of early detection of breast cancer through collaborative multi-country efforts: medical physics component. Phys Med 2018;48:127–34.
[7] IAEA. Quality assurance programme for digital mammography. IAEA Human Health Series No. 17; 2011.
[8] NOM-158-SSA1-1996, Especificaciones técnicas para equipos de diagnóstico médico con rayos X. México: Secretaría de Salud, DOF; 1996.
[9] NOM-229-SSA1-2002, Requisitos técnicos para las instalaciones, responsabilidades sanitarias, especificaciones técnicas para los equipos y protección radiológica en establecimientos de diagnóstico médico con rayos X. México: Secretaría de Salud, DOF; 2006.
[10] NOM-041-SSA2-2011, Para la prevención, diagnóstico, tratamiento, control y vigilancia epidemiológica del cáncer de mama. México: Secretaría de Salud, DOF; 2011.
[11] Brandan M-E, Ruiz-Trejo C, Verdejo-Silva M, Guevara M, Lozano-Zalce H, Madero-Preciado L, et al. Evaluation of equipment performance, patient dose, imaging quality, and diagnostic coincidence in five Mexico City mammography services. Arch Med Res 2004;35:24–30.
[12] Gaona E, Rivera T, Arreola M, Franco J, Molina N, Alvarez B, et al. Exploratory survey of image quality on CR digital mammography imaging systems in Mexico. Appl Radiat Isot 2014;83:245–8.
[13] Leyton F, Nogueira MDS, Dantas M, Duran MP, Ubeda C. Mean glandular dose in six digital mammography services in Santiago, Chile: preliminary reference levels. Radiat Prot Dosimetry 2015;165:115–20.
[14] López-Pineda E, Ruiz-Trejo C, Brandan ME. A mammographic phantom to measure mean glandular dose by thermoluminescent dosimetry. Radiat Meas 2014;71:297–9.
[15] Dance DR, Skinner CL, Young KC, Beckett JR, Kotre CJ. Additional factors for the estimation of mean glandular breast dose using the UK mammography dosimetry protocol. Phys Med Biol 2000;45:3225–40.
[16] Dance DR, Young KC, van Engen RE. Further factors for the estimation of mean glandular dose using the United Kingdom, European and IAEA breast dosimetry protocols. Phys Med Biol 2009;54:4361–72.
[17] Chevalier del Rio M, Núñez de Villavicencio y de Soto MC, Sociedad Española de Física Médica. Protocolo de control de calidad en mamografía digital. Edicomplet; 2008.
[18] SERAM, SEFM, SEPR. Protocolo Español de Control de Control de Calidad en Radiodiagnostico. Senda Editorial S.A.; 2011.
[19] American College of Radiology. Mammography Quality Control Manual. ACR; 1999.
[20] Van der Burght R, Thijssen MBR. Manual contrast-detail phantom CDMAM 3.4 & CDMAM Analyser software V1.2; 2009.
[21] López-Pineda E, Ruiz-Trejo C, Brandan M-E. Image quality and mean glandular dose in Mexican mammography services measured with an Object-Insert/TL mammography kit. AIP Conf Proc 2016:1747.
[22] Fabiszewska E, Grabska I, Pasicz K. The threshold contrast thickness evaluated with different CDMAM phantoms and software. Nukleonika 2016;61:53–9.
[23] Gaona E, Rivera T, Molina-Frechero N, Franco JG. Exploratory survey of initial image quality in new digital mammography units prior to use in patients in Mexico. Appl Radiat Isot 2018;141:266–9.